

Total Propagated Uncertainty (TPU) for Hydrographic LiDAR to Aid Objective Comparison to Acoustic Datasets

By Carol Lockhart, Doug Lockhart and José Martinez, Fugro Pelagos (USA)



Abstracts

Previously, when comparing LiDAR datasets to other LiDAR or acoustic datasets, comparisons have always presumed that one control dataset is ultimately correct, with no errors. All error is attributed to the second dataset. Surface and target analysis methods have therefore been somewhat subjective. The use of TPU takes into account the fact that each depth point is an estimate with an associated uncertainty. This paper discusses a method to derive TPU for LiDAR sensors, so that CUBE may be used to perform an objective comparison of LiDAR bathymetry and acoustic datasets.



Résumé

Auparavant, lorsque l'on comparait des ensembles de données LiDAR à d'autres ensembles de données LiDAR ou acoustiques, on présumait qu'un ensemble de données de contrôle était finalement correct, sans aucune erreur. Toute erreur était attribuée au deuxième ensemble de données. Les méthodes d'analyse de surface et d'objectif étaient toutefois quelque peu subjectives. L'utilisation du TPU prend en compte le fait que chaque point de profondeur représente une estimation à laquelle est associée une incertitude. Cet article traite d'une méthode en vue de dériver le TPU pour les capteurs LiDAR, de façon à ce que CUBE puisse être utilisé en vue d'établir une comparaison objective de la bathymétrie LiDAR et des ensembles de données acoustiques.



Resumen

Previamente, cuando se compara la base de datos LIDAR con otras bases de datos LIDAR o acústicos, las comparaciones siempre presumen que una base de datos de control es finalmente correcta, sin errores. Todo error es atribuido a la segunda base de datos. Los métodos de análisis de blancos y superficie han sido por lo tanto en cierta medida subjetivos. El empleo de TPU toma en consideración el hecho que cada punto de profundidad es una estimación con una incertidumbre asociada. Este artículo discute un método para derivar TPU del sensor LIDAR, de forma tal que CUBE pueda ser empleado para hacer una comparación objetiva de las bases de datos de batimetría LIDAR y acústica.



In August 2007, Fugro Pelagos collected data with the SHOALS-1000T bathymetric LiDAR system in Shilshole Bay, Seattle, for NOAA Office of Coast Survey (OCS). Data were collected at various spot spacings, altitudes, and times of day, over an area previously surveyed with an 8101 multi-beam echo sounder. In addition, the area contained targets of known size, built and placed on the seafloor by Fugro Pelagos in 2005. Data were collected to study the Total Propagated Uncertainty (TPU) of the SHOALS-1000T LiDAR measurements and the system's target detection capabilities.

Target detection tests have been conducted previously over the Shilshole area, for the LADS, SHOALS-400 and SHOALS-1000T sensors (McKenzie et al., 2001; Lockhart et al., 2005). However previous comparisons, have always presumed that the multi-beam control dataset is ultimately correct, with no errors. Therefore, all error is attributed to the LiDAR dataset. Surface and target analysis methods have consequently been somewhat subjective. In addition in areas with many targets, they can become very labour intensive. Target detection for hydrographic surveys is currently specified by the International Hydrographic Organization (IHO) Special Publication No. 44 (IHO, 1998).

The use of Total Propagated Uncertainty (TPU) takes into account the fact that each depth or elevation point is an estimate with an associated measurement uncertainty. These uncertainties can then be used by the Combined Uncertainty and Bathymetry Estimator (CUBE) algorithm developed at the University of New Hampshire (Calder and Mayer, 2001) to build an attributed bathymetry surface: now a required standard deliverable for NOAA OCS. If surfaces can be built, with knowledge of the uncertainty, then there is the potential to use the CUBE algorithm to compare these different density multi-beam and LiDAR datasets more objectively, including for target detection. In theory this would allow the analysis of the final surfaces to see if they represent the same seafloor, and targets, once the uncertainty

of the measurements is taken into account.

Before the CUBE analysis can be conducted however, TPU models must exist for each dataset. Although TPU is now commonly used for multibeam data processing, a TPU model did not exist for the SHOALS-1000T data. Therefore the first step was to develop this uncertainty model.

Data Acquisition

Shilshole Bay in Puget Sound, Washington has been used extensively in the past by NOAA OCS and Fugro Pelagos to conduct multibeam sonar and LiDAR verification surveys. For this study, multibeam data was acquired with a Reson 8101 multibeam echosounder (MBES) in 2005, shortly after manufactured targets were placed on the seafloor. Figure 1 shows a colour-coded DEM of the MBES coverage, the location of the targets and the planned extents of the LiDAR acquisition.

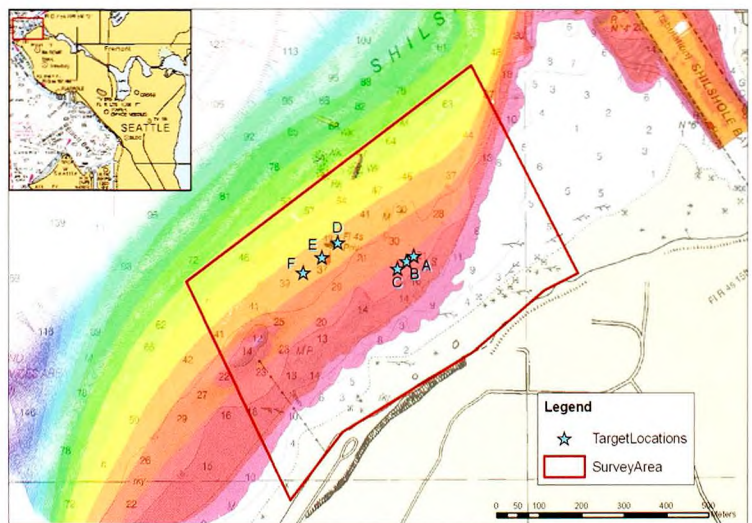


Figure 1: Survey Location, Shilshole Bay, Puget Sound (WA, USA).

The targets themselves are boxes constructed from steel, as shown in Figure 2. Three sizes were constructed: 2x2x2m, 2x2x1m and 1x1x1m. One target of each size was placed in 7m water depth (reduced), and another set of targets was placed at approximately 12.5m water depth, as indicated in Table 1. Although initially reflective, over time these targets reflectivity has become very similar to that of the surrounding seafloor (Figure 2).

Target ID	Target Description	Latitude	Longitude	Approximate Depth (m)
A	2x2x1m	47-40-16.42N	122-25-12.67W	7
B	2x2x2m	47-40-16.06N	122-25-13.47W	7
C	1x1x1m	47-40-15.53N	122-25-14.46W	7
D	2x2x1m	47-40-17.45N	122-25-21.19W	12.5
E	2x2x2m	47-40-16.38N	122-25-23.01W	12.5
F	1x1x1m	47-40-15.25N	122-25-25.10W	12.5

Table 1: Shilshole Target Descriptions.

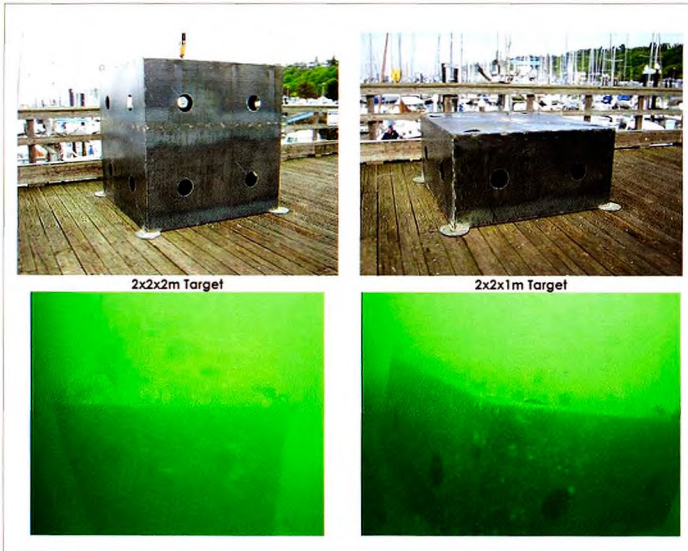


Figure 2: Targets: Constructed and on the Seafloor in December 2007.

mean high water (MHW) line out to the 20m depth contour. The survey limits included the area where targets were set on the seabed in 2005.

Survey flight missions were conducted at various spot spacing, flight altitudes, flight line directions and time of the day as shown in Table 2. In all instances lines were planned with 20% overlap. These multiple datasets were collected so that percentage of data coverage (i.e. 100%, 200%, 300%, etc...), flight altitude, flight direction and time of day could be assessed to see how each factor may or may not affect bathymetric LiDAR target detection.

The SHOALS-1000T survey took place on 27 to 29 August 2007 during which the following data were collected:

- Bathymetric LiDAR data from the SHOALS-1000T
- Digital Aerial Photography from the SHOALS-1000T
- GPS Ground Control

A complete description of the SHOALS-1000T can be found in Guenther et. al. *Meeting the Accuracy Challenge in Airborne Lidar Bathymetry*. This document is generally available on line.

The hydrographic LiDAR flight lines were planned to collect data from the approximate location of the



Figure 3: SHOALS-1000T as installed. The operator console is to the left, power and cooling are in the center stack, and the laser, IMU and camera are to the right.

Mission	Spot Spacing (m ²)	Altitude	Direction	Time of Day
1	3x3	400m	E → W	Day
2	3x3	400m	W → E	Day
3	3x3	400m	E → W	Day
4	3x3	400m	E → W	Night
5	3x3	400m	W → E	Night
6	3x3	300m	E → W	Night
7	3x3	300m	W → E	Night
8	2x2	400m	E → W	Day
9	2x2	400m	W → E	Day
10	4x4	400m	E → W	Day
11	4x4	400m	W → E	Day

Table 2: Bathymetric LiDAR Acquisition Missions

LiDAR Data Processing

Raw SHOALS-1000T data from the airborne system were downloaded into the Optech SHOALS

Ground Control System (GCS) on Windows XP workstations. GCS includes links to Applanix POSPac software for GPS/inertial processing and to IVS Fledermaus software for data visualization and 3D editing. GCS was used to apply the KGPS/inertial solutions, apply tide data, auto-process the LiDAR waveforms, edit data and export point cloud files to ASCII XYZ format files. The ASCII XYZ files were used for TPU calculations.

Edited data were also imported to CARIS HIPS for analysis with the CUBE algorithm.

In order to assess the affect of data coverage percentage, flight altitude, flight direction and time of day, on target detection, flight missions were organized into processing datasets (Table 3) prior to

data editing,. Each dataset was processed independently, so that the data editor did not gain additional knowledge by looking at all flight missions at once.

Dataset	Missions Included
A	400 m @ 3x3 200% coverage with flight in opposite directions
B	400 m @ 3x3 200% coverage with flight in same directions
C	400 m @ 3x3 200% coverage with flight in opposite directions at night
D	400 m @ 3x3 300% coverage
E	400 m @ 3x3 400% coverage
F	400 m @ 3x3 500% coverage
G	300 m @ 3x3 200% coverage with flight in opposite directions
H	400 m @ 2x2 200% coverage with flight in opposite directions
I	400 m @ 4x4 200% coverage with flight in opposite directions

Table 3: Processing Datasets.

Derivation of SHOALS-1000T TPU Model

The TPU can be understood as the sum of all random and systematic uncertainties in the measurement process, including the uncertainty contribution of all sensors embedded in the SHOALS-1000T system. Determining each sensor’s uncertainty independently to develop a TPU is a work in progress. Due to the complexity of the physical interaction of the laser pulse with the sea surface, sea water and sea floor an analytical TPU may not be possible. Therefore, at this time, an alternate method must be used to derive a TPU estimate for the SHOALS 1000T system.

This study uses depth variance as a proxy for an analytical TPU. Because the bathymetric LiDAR footprint spreads with depth, as the light scatters and absorbs in the water column, the SHOALS data were separated into ASCII XYZ files with discrete depth ranges, starting at 2m water depth down to 16m, at 2m step increments. For each depth interval, variance is estimated as a function of horizontal radius. This variance function is then calculated for a radius of zero giving vertical variance for that depth interval.

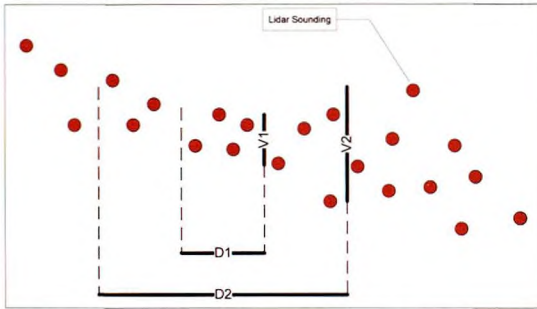


Figure 4: Variance as a function of distance.

Figure 3 shows the increase in variance with increased radius of investigation. The red dots show sounding depths and there is an apparent slope from left to right. In this study, the variance is initially assumed to be isotropic; and assumption that is clearly in error. Slopes and other features such as sand waves will result in anisotropic variances. An effort is made at a later step to identify and account for geographically associated anisotropy. There is no effort in this study to identify instrument based anisotropy. For all depth intervals, total variance is expected to grow with each incremental search radius; however, variance growth as a function of distance, defines a function that allows the estimation of variance at

zero radius, which cannot be resolved directly. A variogram is used to determine the node variance when the constant of a polynomial fit is found, as shown in Figure 5. Variance functions for each depth interval are shown in Figure 6.

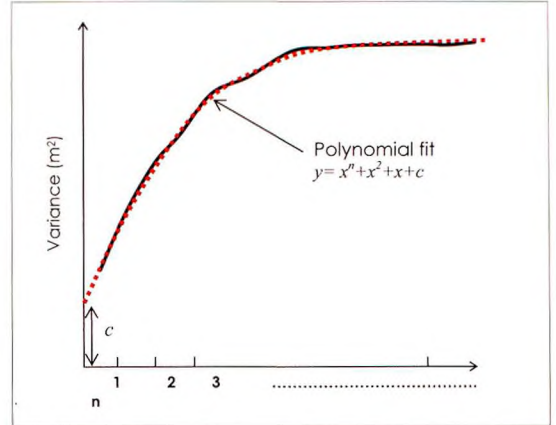


Figure 5: Variogram for Determining Node Variance.

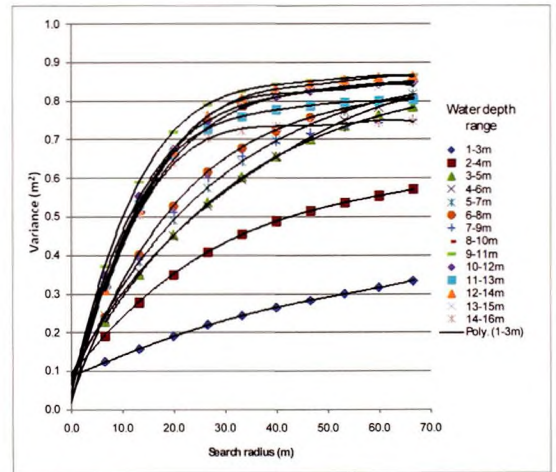


Figure 6: Variance Function for each Depth Interval (including Zero Radius).

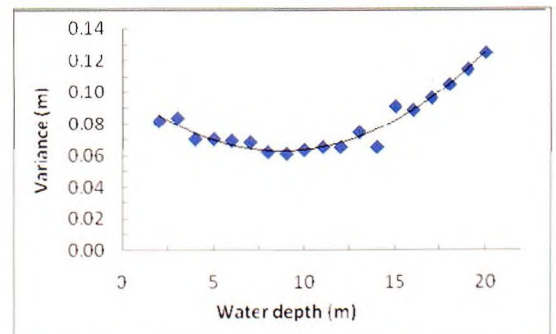


Figure 7: Variance as a Function of Water Depth.

Calculated node variances for each depth interval are shown in Figure 7. From this, one can see that variance fluctuated between 0.07-0.09m to 15m water depth and then grew to about 0.125 m at 20m water depth.

This total variance estimate (σ_T^2) calculated as described above, includes the variance from the sensor measurements as well as the variance inherent in the seafloor (σ_s^2) due to slope and roughness. Therefore to produce an estimate of sensor measurement variance (σ_m^2), an estimate of seafloor variance needs to be calculated or modeled and removed from the total variance, as presented in the form:

$$\sigma_m^2 = \sigma_T^2 - \sigma_s^2$$

To model the natural seafloor variance in the LiDAR data, introduced by slope and bottom roughness, a morphology trend was observed and determined from the gridded multibeam DEM surface. The slope gradient, and the amplitude and frequency of the general bottom roughness, were used in the creation of a synthetic surface grid model. Variance analysis was conducted on the synthetic surface using the variogram approach to provide an estimate of variance solely from the slope and bottom roughness. Different synthetic surface point densities (0.5m, 1m, 2m and 3m) were used to account for potential sub-sampling effects. Figure 8 shows the results of the synthetic surface variance analysis showing clearly that variance as function of distance remains constant and follows a linear trend not affected by different point density. It was found that the variance for the modeled synthetic seafloor averaged 0.015m. However, due to the use of a synthetic sur-

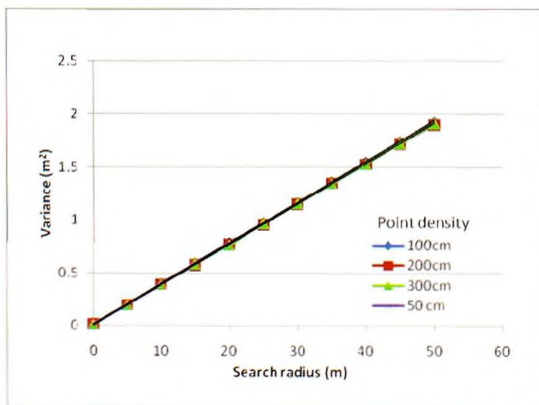


Figure 8: Variance of the Synthetic Seafloor at Varying Point Density.

face, it is likely that this is a low estimation of actual seafloor variance. Estimated seafloor variance was then removed from the total variance to provide an estimate of the sensor variance. The square-root of final sensor variance (standard deviation) was then used as the TPU estimate, with the value varying dependent on water depth.

Table 4 shows the calculated TPU for the Shilshole Bay survey, where maximum bottom depth detection was at about 16 meters. TPU was attributed to each LiDAR depth in CARIS HIPS and used to create attributed uncertainty DEM products.

It should be noted that uncertainty calculated still includes any uncertainty present from the tide application. It would be beneficial to repeat this exercise using PPK GPS LiDAR data on the ellipsoid, to provide a result which more closely represented the sensor uncertainty alone.

Table 4 also shows for comparison the depth accuracy specification for IHO Order 1 given, in the form:

$$D_a = \sqrt{a^2 + (bx)^2}$$

where D_a is water depth, and values for a and b are 0.5 m and 0.013 m, respectively.

Comparing numbers in columns 5 and 6, it can be deduced that accuracy for the SHOALS-1000T bathymetric LiDAR depths in Shilshole Bay are within the acceptable accuracy limits of IHO Order 1.

It is important to note that TPU estimation using the method presented above is valid for the water conditions at the time of the survey. Bathymetric LiDAR measurement uncertainty will vary depending on local water column conditions and seafloor reflectance. In this study, what we are calculating can be better described as a local estimate of TPU. We do not have enough data from one survey to sample the entire bandwidth of the uncertainty. If water conditions and depth of bottom detection are very similar in other locations sharing common environments, this model can be applied. To use in a different environment, TPU would need to be recalculated using this same method.

This method can also be refined by the use of Kriging, which will allow uncertainty relationships in the along-track and across-track direction to be modeled. This is currently being examined by Fugro Pelagos.

1	2	3	4	5	6	7	8	9
Depth (m)	Total Seafloor Variance (σ_T^2) m ²	Synthetic Seafloor Variance (σ_s^2) m ²	Sensor Variance (σ_m^2) m ²	Sensor Variance of a Mean ($\sigma_m^2/\sqrt{2}$) m ²	Sensor StDev (σ_m) TPU m	Sensor 2-StDev m	IHO Order 1 (2-StDev) m	Status
1	0.094	0.015	0.079	0.056	0.236	0.472	0.500	Passed
2	0.083	0.015	0.068	0.048	0.219	0.439	0.501	Passed
3	0.085	0.015	0.070	0.049	0.222	0.445	0.502	Passed
4	0.072	0.015	0.057	0.040	0.201	0.402	0.503	Passed
5	0.072	0.015	0.057	0.040	0.201	0.402	0.504	Passed
6	0.071	0.015	0.056	0.040	0.199	0.398	0.506	Passed
7	0.070	0.015	0.055	0.039	0.197	0.394	0.508	Passed
8	0.064	0.015	0.049	0.035	0.186	0.372	0.511	Passed
9	0.063	0.015	0.048	0.034	0.184	0.368	0.514	Passed
10	0.065	0.015	0.050	0.036	0.189	0.377	0.517	Passed
11	0.067	0.015	0.052	0.037	0.192	0.383	0.520	Passed
12	0.067	0.015	0.052	0.037	0.192	0.384	0.524	Passed
13	0.076	0.015	0.061	0.043	0.208	0.415	0.528	Passed
14	0.067	0.015	0.052	0.037	0.192	0.384	0.532	Passed
15	0.092	0.015	0.077	0.054	0.233	0.467	0.537	Passed
16	0.090	0.015	0.075	0.053	0.230	0.460	0.542	Passed

Table 4: Final Sensor Variance and TPU Values Compared to IHO Order 1.

Using CUBE to Identify Targets in LiDAR Data

CUBE transforms measured points at relatively random locations into regularly spaced depth estimates in a grid. On each grid node, four values are produced: depth, uncertainty (from depth TPU), number of hypothesis and hypothesis strength. Depending on how close or sparse vertically contributing depths are to resulting node value, the algorithm develops more than one potential depth candidate but selects one as the most likely one.

CUBE was designed to aid in the processing of dense multibeam echosounder datasets. However it is not commonly used on sparser bathymetric LiDAR datasets. Some experiments were run to identify suitable CUBE parameters to be used with the LiDAR data points. In the example below (Figure 9), which shows 400% LiDAR coverage, there are 5 LiDAR hits on the target. CUBE successfully generates a likely primary hypothesis (green cubes) from these

5 data points which represent the target. However the primary hypothesis representing the target is relatively weak. The cubes in the image indicate the uncertainty of the measurement in the vertical, with the strength of the hypothesis indicated by the width of the cubes. The CUBE algorithm also generates an alternate hypothesis, shown by the red cubes.

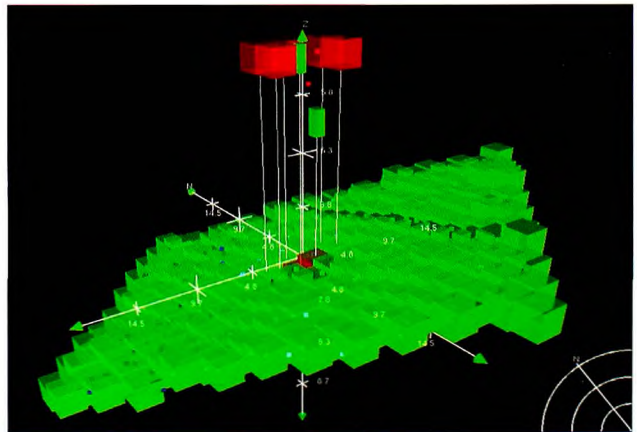


Figure 9 - CUBE Hypotheses for Target B (2x2x2m) in 7m Water Depth with 400% Coverage

In almost all cases, when LiDAR acquired a data point on a target, CUBE correctly created a primary hypothesis, which in some way represented that target. This is likely due to the sparseness of the data, which in many cases with 200% LiDAR coverage or less, prevents the possibility of multiple hypotheses. However the primary hypothesis over the targets was usually weak. In a typical product flow, the primary CUBE hypothesis is then used to create a surface. But if the hypothesis is weak, the surface will not be 'pulled' to the top of the target and will not therefore accurately represent the shallow data points. Further work is still required in order to identify a set of CUBE parameters that will provide a strong primary hypothesis on the targets when they are observed in the LiDAR data.

Conclusions

TPU can be estimated for LiDAR depth intervals through variance node analysis. The analysis can be performed over a small control area in water conditions very similar to the actual main survey area, and therefore could be calculated on a project-by-project, or area-by-area basis.

The calculated TPU presented here for Shilshole Bay still includes any uncertainty present from the tide application to the LiDAR data. It would be beneficial to repeat this exercise using PPK GPS LiDAR data on the ellipsoid, to provide a result which would more closely represent the sensor uncertainty alone.

This methodology for calculating TPU should be further refined and automated with the use of Kriging. At the time of writing, CUBE has not been successfully used to compare the LiDAR and multibeam datasets. However the authors feel that with further effort, particularly in choosing suitable CUBE parameters for LiDAR and multibeam hypothesis selection, this can be accomplished.

Acknowledgements

This work was accomplished under NOAA contract OPR-0180-KRL-07 for LiDAR Survey Services in Keku Strait, Alaska. The authors and Fugro Pelagos Inc. appreciate and thank the NOAA's Office of Coast Survey for its continued support and interest in hydrographic LiDAR survey services.

References

- Lockhart, C., Arumugam, D., Millar, D., 2005. *Meeting Hydrographic Charting Specifications with the SHOALS-1000T Airborne LiDAR Bathymeter*, Proceedings of the 2005 U.S. Hydrographic Conference, San Diego (CA, USA)
- McKenzie, C., Gilmour, B., Van Den Ameele, E.J., Sinclair, M. 2001. *Integration of LiDAR Data in CARIS HIPS for NOAA Charting*. Proc. The 6th Annual International CARIS Users' Conference, October 30 – November 2, 2001. San Diego (CA, USA)
- Calder B. and Mayer, L.A.. 2001. *Robust Automatic Multibeam Bathymetric Processing*. Proceedings of the 2001 U.S. Hydrographic Conference, Norfolk (VA, USA)
- Guenther, G., Cunningham, G., LaRocque, P, Reid, D., *Meeting the Accuracy Challenge in Airborne lidar Bathymetry*, Proceedings of EARLSel-SIG-Workshop LIDA, Dresden/FRG, June 16-17, 2000
- International Hydrographic Organization. 1998. *IHO Standards for Hydrographic Surveys*. Special Publication No. 44. 4th Edition, April 1998. Monaco.
- Taylor, B., Kuyatt, C., *Guidelines for evaluation and expressing the Uncertainty of NIST Measurement Results*, United States Department of Commerce Technology Administration, National Institute of Standards and technology. NIST Technical Note 1297, 1994 Edition.
- Carol Lockhart** is the LiDAR Technical Manager at Fugro Pelagos in San Diego, California. She received her B.Sc. (Hons) degree in Topographic Science (Geomatics) from the University of Glasgow. She is responsible for the technical management of LiDAR activities and has been involved in developing Fugro Pelagos' hydrographic capability for the last 12 years.
- Doug Lockhart** is the Chief Scientist at Fugro Pelagos in San Diego, California. He has B.S and M.S degrees in Petroleum Engineering from the University of Alaska, Fairbanks. He has been actively involved in the development and implementation of

high resolution geophysical and hydrographic acquisition and processing techniques for 15 years.

Jose Martinez is the LiDAR Processing Manager at Fugro Pelagos. He received his M.Eng. (Geo-

omatics) from the University of New Brunswick and B.Sc. (Oceanography) from the Universidad A. de Baja California. He has worked with Fugro Pelagos in his hydrographic surveying capacity for the last 8 years.